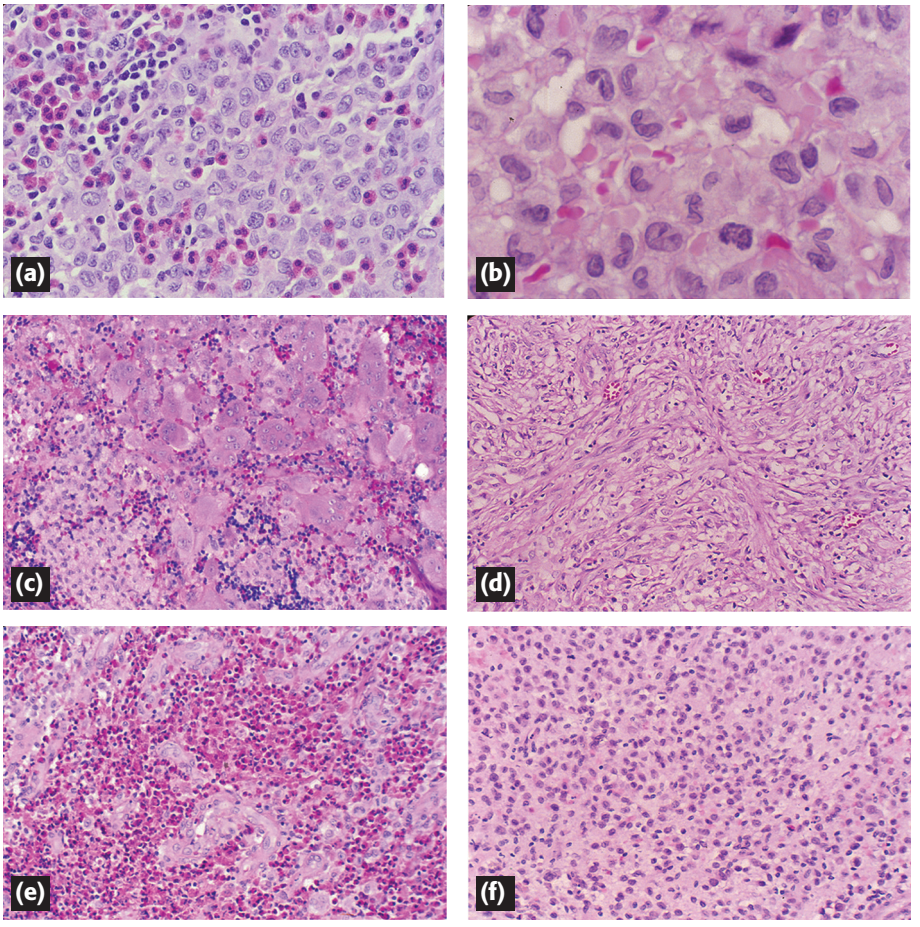

Fig. 2.1 LCH histology. (a) LCH in its most classical form has sheets of cytoplasm-rich pale histiocytes interspersed with inflammatory cells, eosinophils and lymphocytes. (b) Nuclear morphology is typical and consists of monocytoid, grooved and complexly folded forms in a pale-staining cytoplasm. (c) Giant cells can be of different types. Osteoclast-like giant cells are most common in and around bone lesions. This picture shows osteoclast-type giant cells with multiple round nuclei in a lymph node. (d) LCH can adopt a spindle-cell form. The LCH phenotype of these spindled forms is preserved. (e) Eosinophils can be overwhelming, forming eosinophilic micro-abscesses that contain Charcot–Leyden crystals. (f) Eosinophils are not a required component. Some lesions are devoid of eosinophils (same patient as Figure 2.1(e))

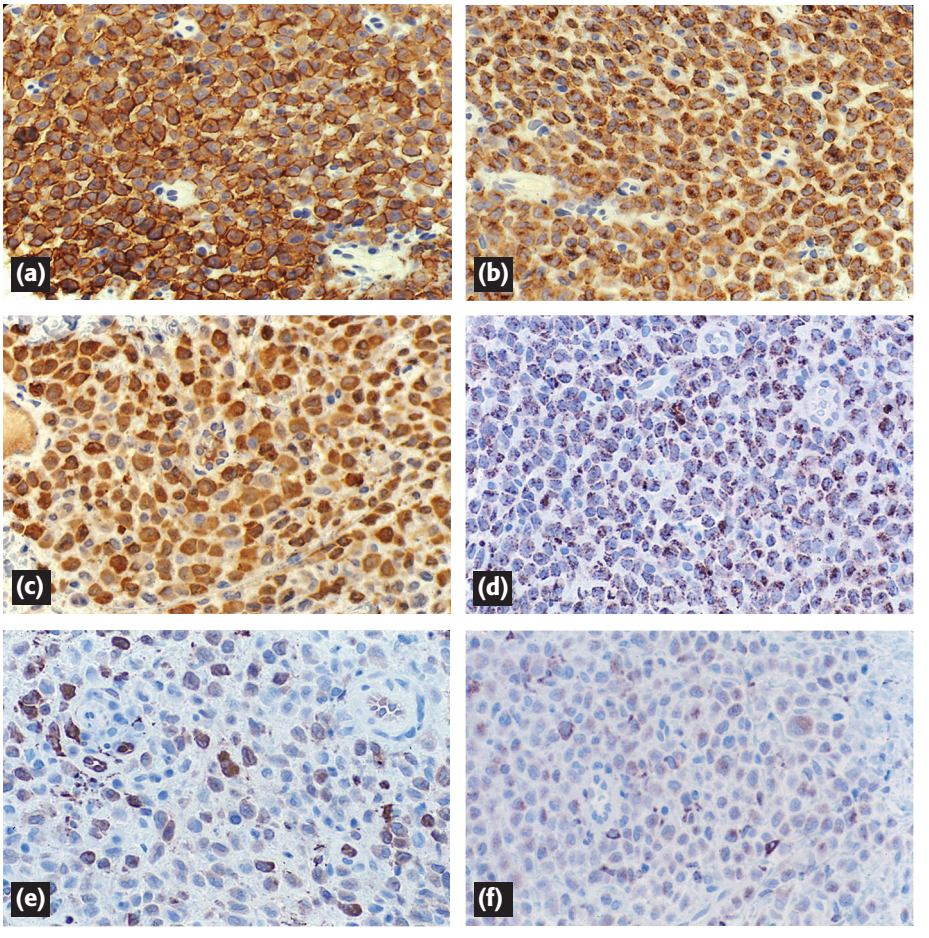

Fig. 2.3 LCH prototypical phenotype. (a) The LCH cells have surface and some paranuclear staining for CD1a. (b) Granular cytoplasmic staining for Langerin. (c) Diffuse cytoplasmic/nuclear staining for S100. (d) HLA Class II (LN3 antibody) reveals intracytoplasmic, often paranuclear staining. (e) Fascin is variable and ranges from none to light staining on a minority of cells. (f) CD68, KP-1 antibody, has light granular cytoplasmic staining only

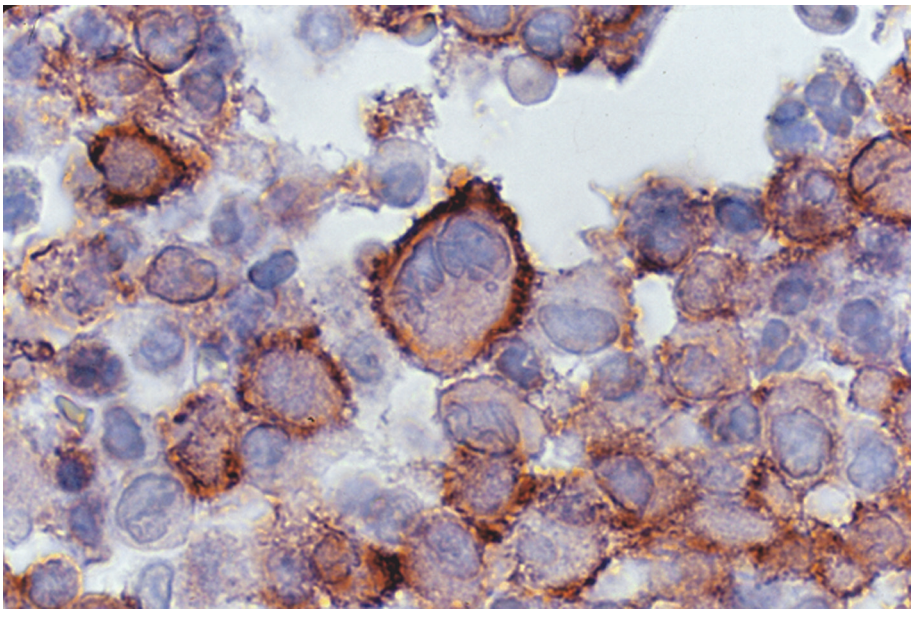

Fig. 2.2 LCH giant cells. Giant and multinucleated forms can occur by cell fusion of LCH cells. A binucleated cell has classical complex LCH nuclei and strong surface CD1a staining. Most giant cells are CD1a−

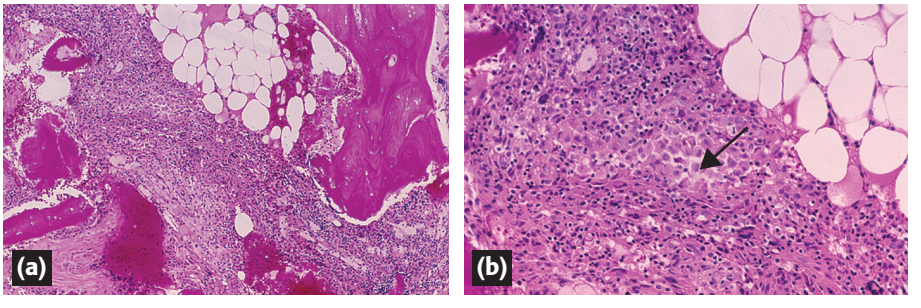

Fig. 2.4 LCH bone, regressing. LCH lesions of bone can appear like those in Figure 2.1 in the active phase. (a) In the regressing phase there is progressive fibrosis, scarring and involution of the LCH cells. (b) The cluster of cells (arrow) was the only residual found after two unsuccessful needle biopsies

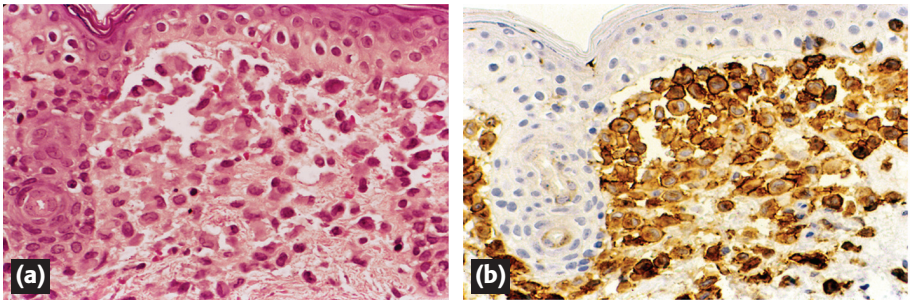

Fig. 2.5 LCH of skin. LCH is described as 'epidermotropic' and fills the papillary dermis in classical LCH. Note (a) that the LCH cells are oval to round not dendritic and (b) that the CD1a+ infiltrate is not perivascular (see also Figure 2.6(f))

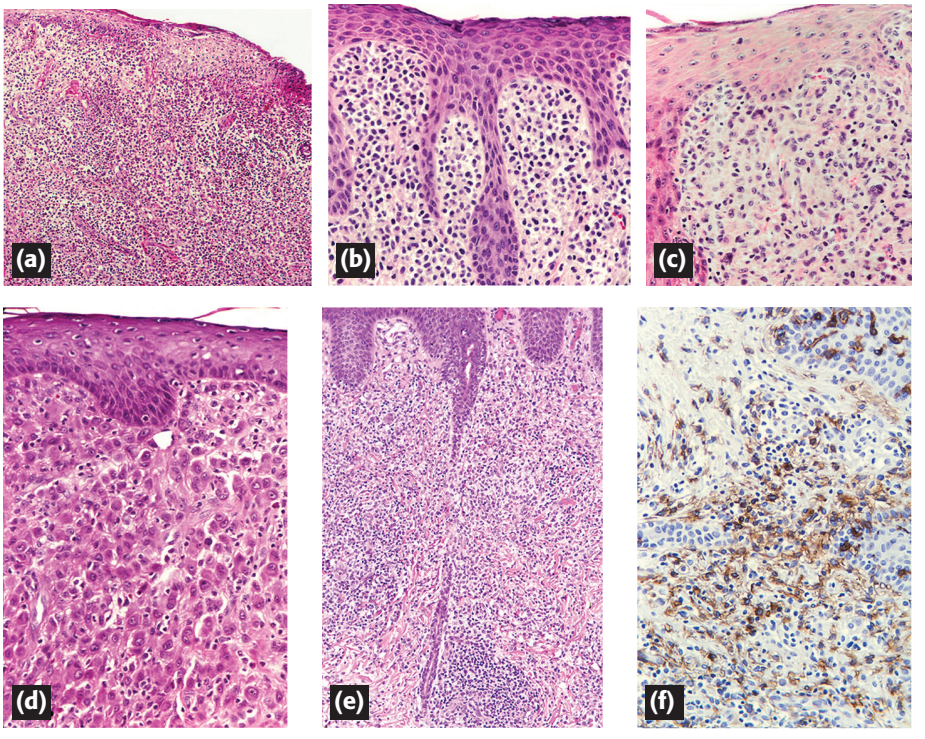

Fig. 2.6 Skin, LCH and look-alikes. (a) Congenital LCH, papular and ulcerated lesion, fills the dermis to the sub-dermal fat. (b) Urticaria pigmentosa. The epidermal saw-tooth hyperplasia and rounded papillae are a feature of mast cell lesions that lack the nuclear complexity. (c) JXG can look very similar when Touton cells are not prominent and can even have a high content of CD1a cells in the sub-epidermal area. Phenotyping (S100−/FXIIIa/fascin/CD163) may be required. (d) Solitary reticulohistiocytomas can be congenital and have large cells with abundant cytoplasm that contain round nuclei with prominent nucleoli. (e) and (f) Some chronic dermatitides contain a substantial dendritic-cell component (S100+/CD1a+). The DCs in these conditions are perivascular in distribution (e) and are generally spindled or dendritic in shape (f) (CD1a stain), unlike LCH cells (see Figure 2.5(a))

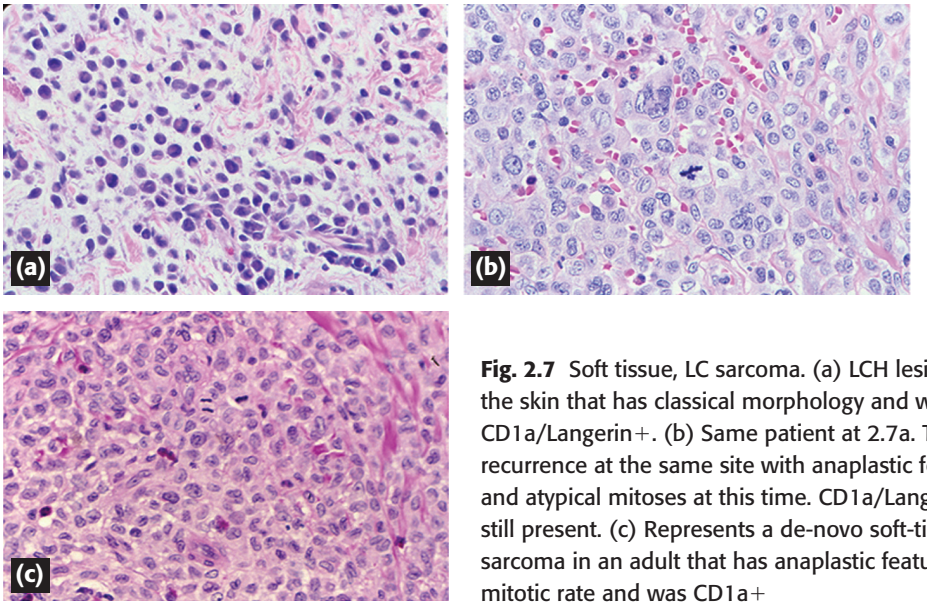

Fig. 2.7 Soft tissue, LC sarcoma. (a) LCH lesion of the skin that has classical morphology and was CD1a/Langerin+. (b) Same patient at 2.7a. The fifth recurrence at the same site with anaplastic features and atypical mitoses at this time. CD1a/Langerin were still present. (c) Represents a de-novo soft-tissue sarcoma in an adult that has anaplastic features, high mitotic rate and was CD1a+

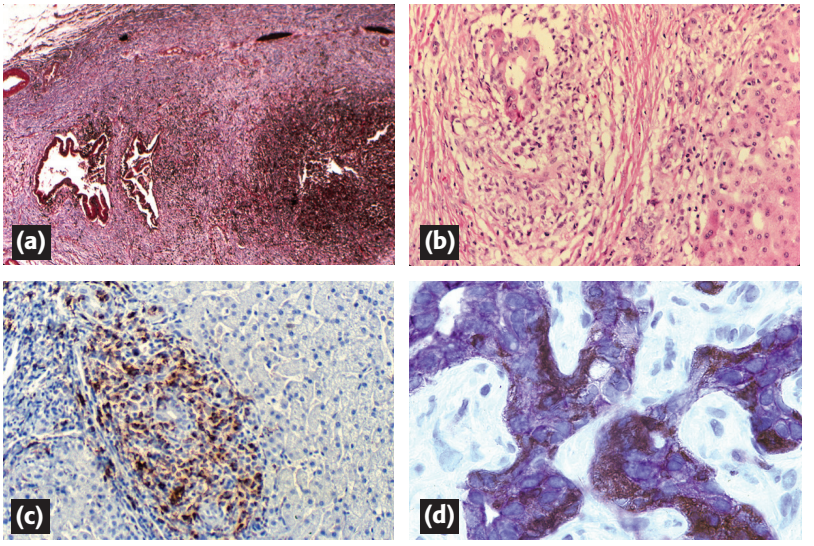

Fig. 2.9 LCH in the liver. (a) The extra-hepatic biliary tree and major bile ducts may be a site of predeliction for LCH involvement of the liver (S100). (b) Intra-hepatic bile ducts can have epithelial damage, periductal LCH infiltration and concentric fibrous scarring. (c) Langerin staining reveals the portal nature of the infiltrate centered around a bile duct. (d) Double-staining with CD1a (black) and cytokeratin (blue) shows the LCH cells in black as they infiltrate proliferating bile ductules and remain confined within the biliary basement membrane. LCH cells can be overlooked unless immunostains are used

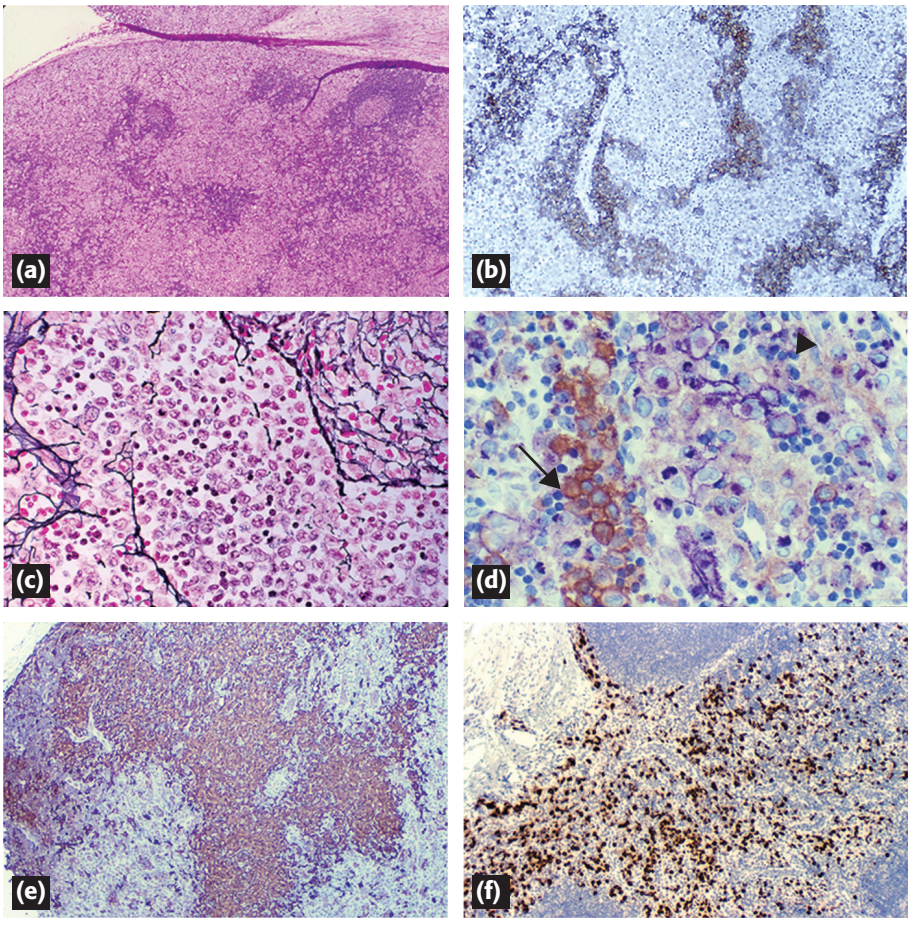

Fig. 2.8 LCH in the lymph node. (a) The lymph node that harbors LCH appears to be filled with LCH cells and only residual follicles are recognized. (b) CD1a immunostain in lymph node highlights cells in the sinuses. Paracortical cells fail to stain for CD1a even though they appear to be similar in appearance. (c) Reticulin stain confirms that much of the LCH infiltrate lies within distended sinuses. (d) Paracortical areas double-stained for CD1a (brown) and HLA-11 (LN3, blue) show that CD1a brown-stained LCH cells in clusters fill sinuses (arrow) while many of the paracortical cells express high levels of HLA-11 on their surface and in paranuclear zones (arrow head) CD1a is presumably lost as these cells 'mature'. (e) and (f) Dermatopathic lymphadenopathy can be confused with LCH because of the high content of (e) CD1a and (f) Langerin cells. A high content of fascin-staining cells that are not sinus in distribution distinguishes dermatopathic nodes from LCH

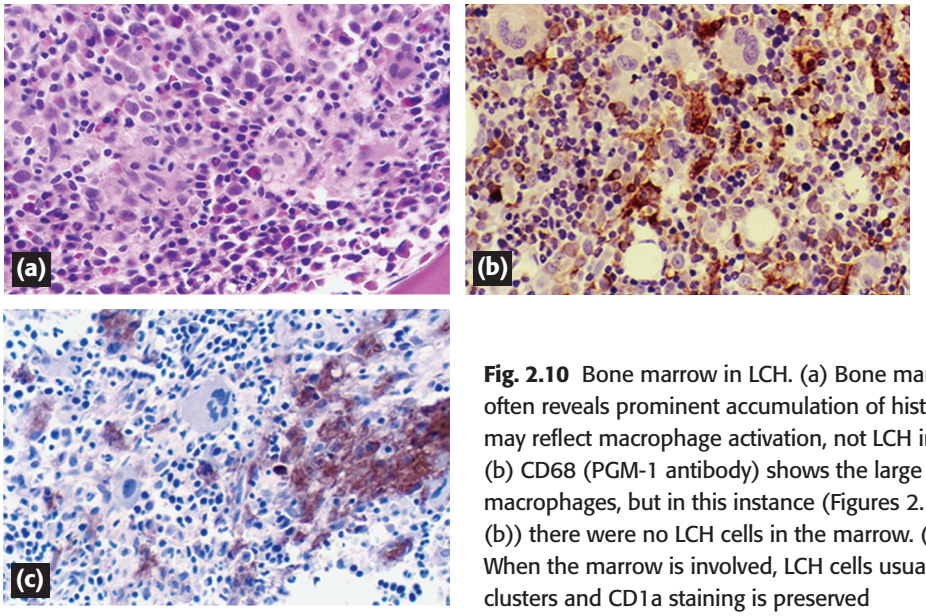

Fig. 2.10 Bone marrow in LCH. (a) Bone marrow in LCH often reveals prominent accumulation of histiocytes. This may reflect macrophage activation, not LCH infiltration. (b) CD68 (PGM-1 antibody) shows the large numbers of macrophages, but in this instance (Figures 2.10(a) and (b)) there were no LCH cells in the marrow. (c) CD1a. When the marrow is involved, LCH cells usually occur in clusters and CD1a staining is preserved

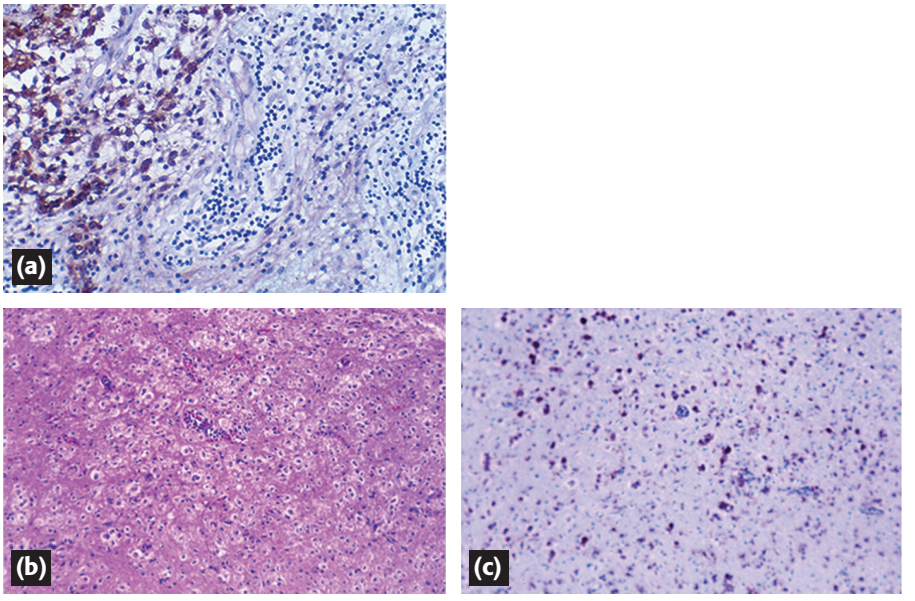

Fig. 2.11 LCH in the brain. (a) Posterior-pituitary and hypothalamic lesions represent LCH infiltration and the cells can be identified (CD1a). (b) and (c) By contrast, the late 'demyelinating' type lesions like this one in the cerebellum do not have identifiable infiltrate (b) and the high content of microglial macrophages is highlighted by CD68 (c)

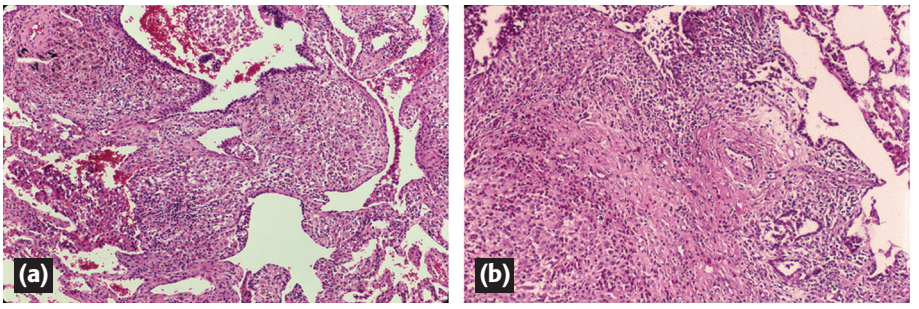

Fig. 2.12 LCH and the lung. (a) Infiltrating LCH cells form nodular aggregates around the airways extending out into adjacent alveolar walls in the active disease. (b) Later effects include the obliteration and scarring of the airways with surrounding inflammatory cells but the sparse LCH cells may be hard to identify

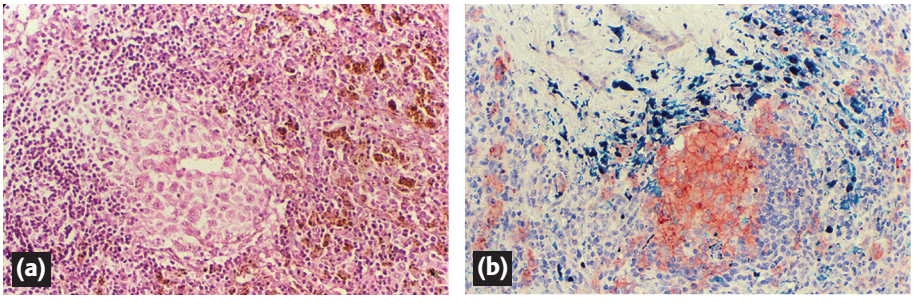

Fig. 2.13 LCH in the spleen. (a) Infiltration of LCH cells is at the margins of the white pulp extending into the red. Hemosiderin can mask the infiltrate and the common presence of macrophage reaction can obscure them. (b) CD1a immunostain (red) in the presence of an iron counterstain (blue) confirms the clusters of LCH cells

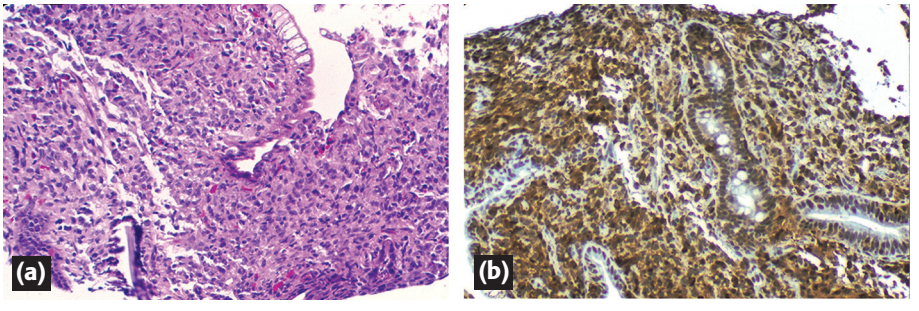

Fig. 2.14 LCH and the intestine. (a) LCH infiltration involves and can fill the lamina propria with superficial epithelial damage. (b) S100 immunostain confirms the nature of the infiltrate

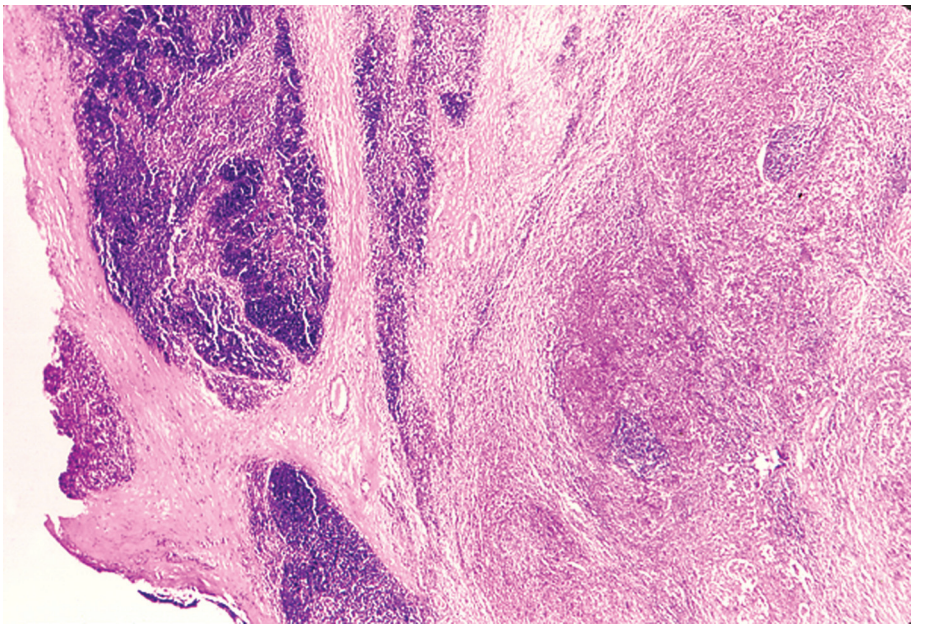

Fig. 2.15 Thymic LCH. LCH in the thymus forms eosinophilic granulomas similar to those at soft-tissue sites and there is often reactive cystic change of the thymus

Fig. 7.1 Necrotic papule in a 3-month-old baby with congenital self-healing reticulohistiocytosis

Fig. 7.2 Ulceration, petechiae and papules in 6-month-old baby with disseminated LCH

Fig. 7.3(a) Neonate born with deep ulceration on cheek

Fig. 7.4 Seborrheic pattern of histiocytosis with petechiae at peripheral edge

Fig. 7.5 Petechial papules diagnostic of LCH

Fig. 7.6 Scattered petechiae in LCH in diaper area

Fig. 7.7 Deep hemorrhagic bulla in a child with skin-only LCH who later progressed to fatal MS disease

Fig. 7.8 Typical deep seborrheic pattern of LCH in diaper area

Fig. 7.9 LCH crusting and petechiae on scalp

Fig. 7.10 Micronodular lesions of JXG

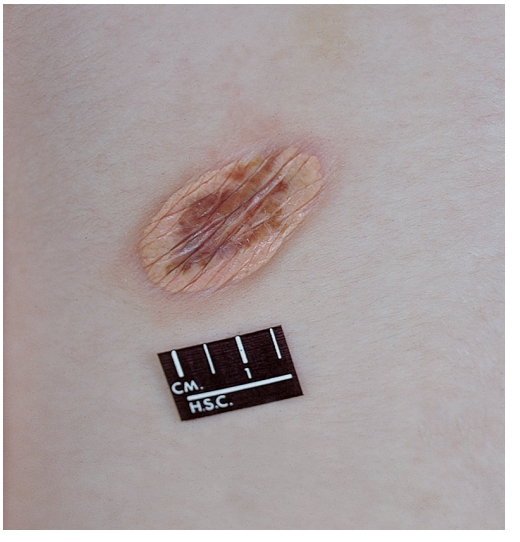

Fig. 7.13 Wrinkling after disappearance of large JXG

Fig. 7.14 Xanthogranuloma: a typical red-yellow nodule

Fig. 7.15 Adult with skin LCH. (a) Involving scalp, (b) vulva and (c) axillary lesion (Figures courtesy of Algin B. Garrett, MD., Richmond, VA.)

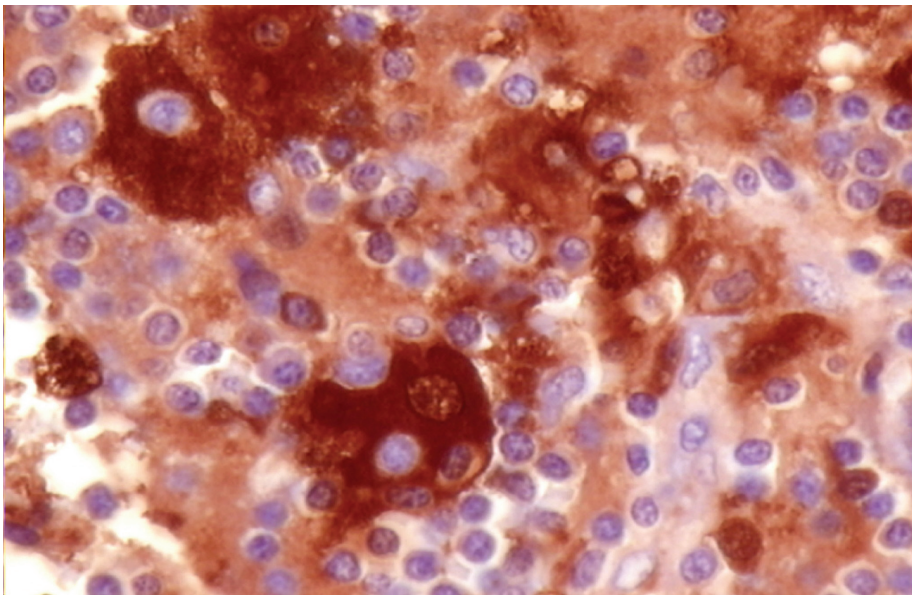

Fig. 15.10 SHML-sinus histiocytes staining positive with S100, showing emperipolesis

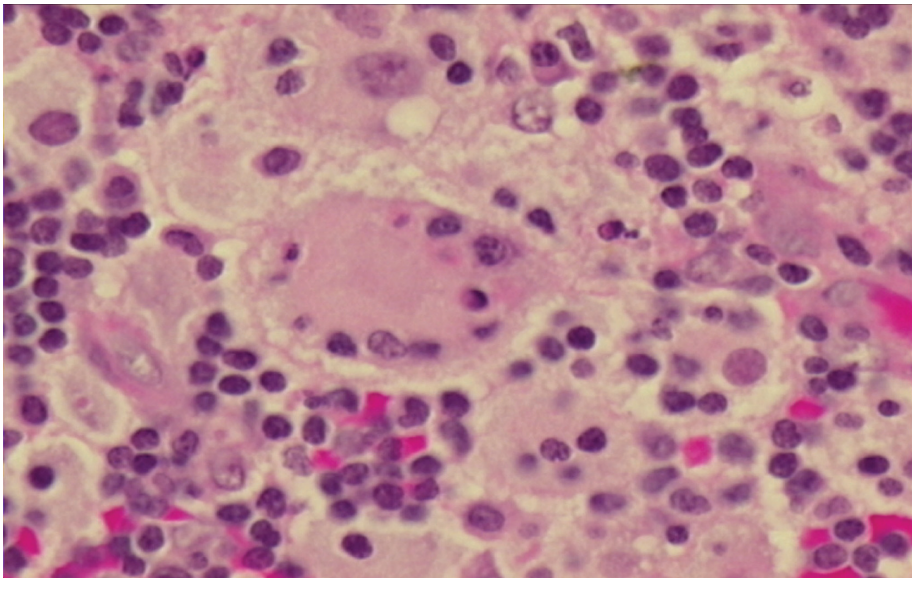

Fig. 15.11 SHML-sinus histiocytes with emperipolesis

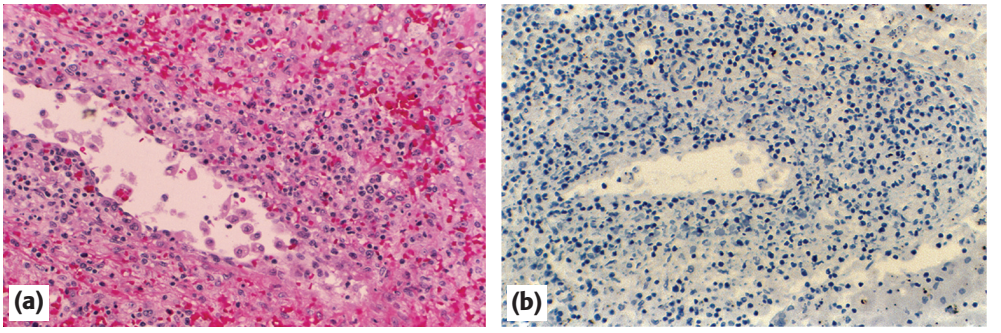

Fig. 16.1 Liver. (a) A lymphohistiocytic infiltrate is present. The presence of the large 'floating' macrophages within portal and central veins is characteristic but not invariable. (b) The infiltrate has no immunostaining for perforin in FHL-2 (perforin, diaminobenzidine (DAB))

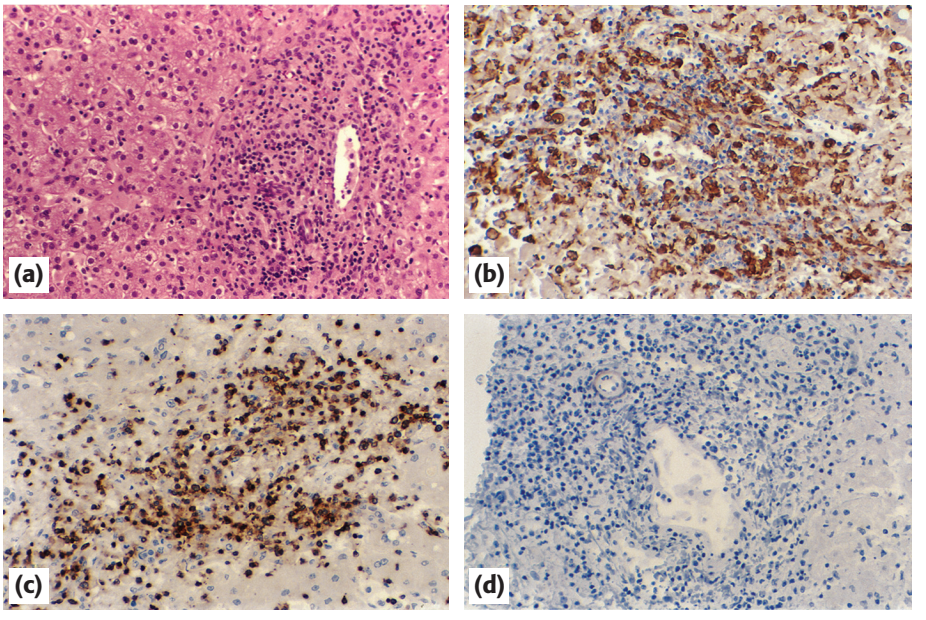

Fig. 16.3 Liver. (a) A mixed lymphohistiocytic infiltrate is concentrated on the portal areas. The large, pale, 'floating' macrophages are noted in a portal vein. (b) Immunostain for the macrophage marker CD163 reveals the extensive portal (and sinusoidal) macrophage infiltrate (diaminobenzidine (DAB)). (c) CD3 stain reveals that the vast majority of the lymphocytes are T-cells (DAB). (d) Perforin immunostain is negative in FHL-2 but not in the other variants or in cases of hepatitis in which many of the T-cells contain perforin

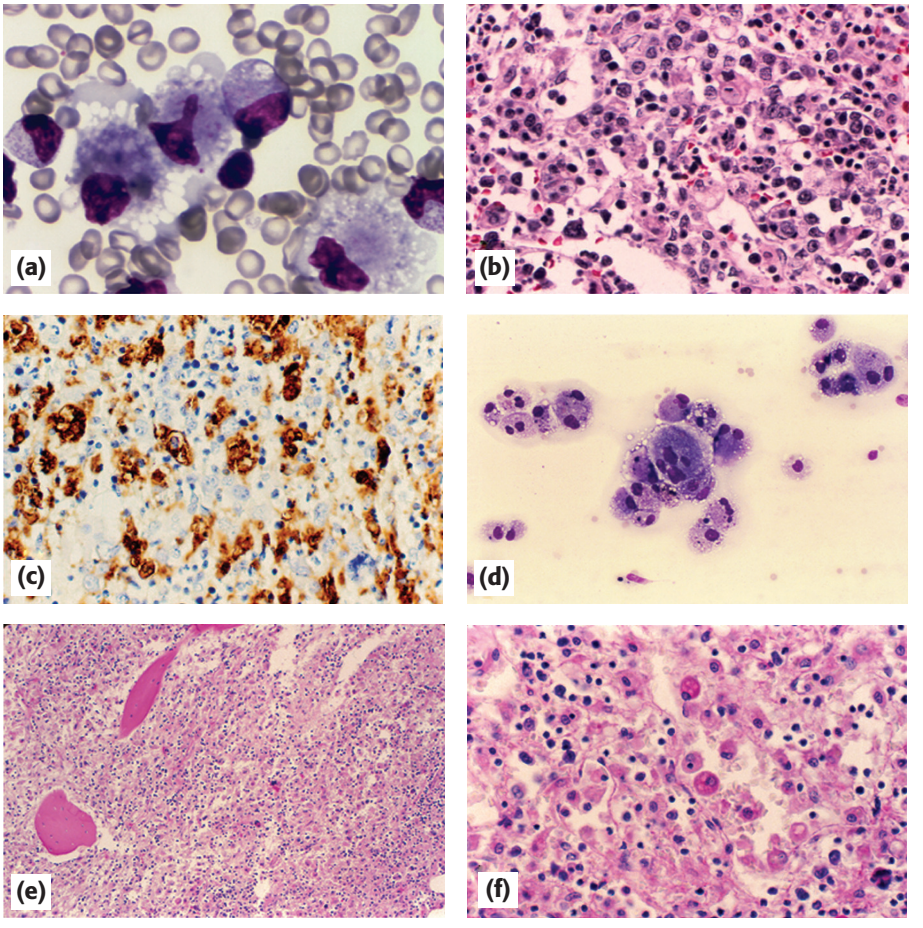

Fig. 16.2 Bone marrow. (a) The aspirate reveals large, cytoplasm-rich macrophages that have cytoplasmic pigment, vacuoles and cell remnants, most commonly erythroid. (b) The biopsy in early active disease contains scattered large and vacuolated macrophages that do not stand out. (c) These macrophages are best seen with anti-CD68 or CD163 staining (CD68, PGM-1, diaminobenzidine (DAB)). (d) Aspirate in late disease (autopsy) may show large numbers of macrophages in the absence of other hematopoietic elements. (e) Bone marrow at autopsy may show vast numbers of large macrophages and only sparse hematopoiesis in a damaged matrix. (f) Periodic acid and Schiff base (PAS) stain reveals the large macrophages, some in dilated vascular sinuses (PAS)

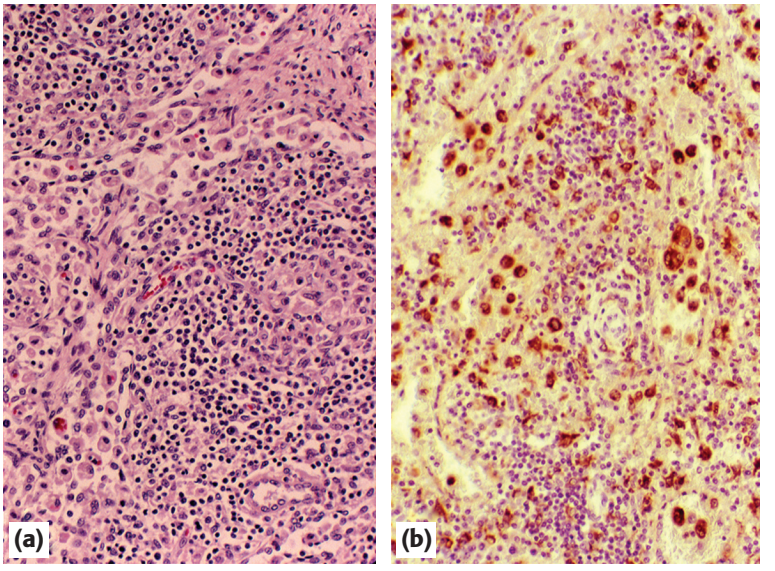

Fig. 16.4 Lymph node. (a) Early active disease is primarily sinus in distribution. Large macrophages, some with hemophagocytosis, fill the sinuses. (b) CD68 highlights the large phagocytic cells and their cytoplasmic vacuoles (CD68, KP-1, DAB)

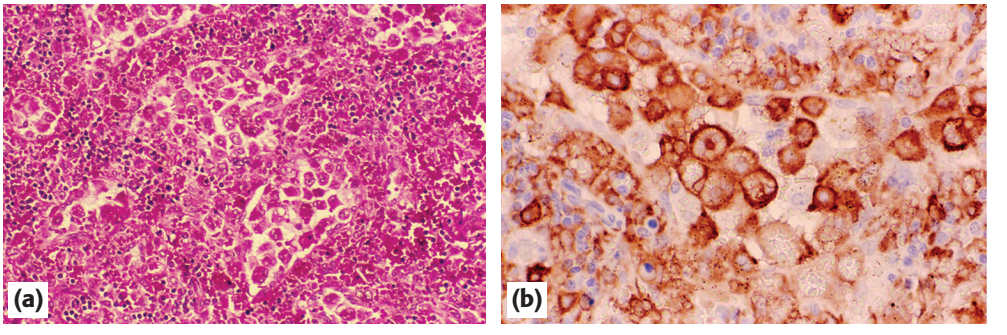

Fig. 16.5 Spleen. (a) The splenic sinuses are filled with large hemophagocytic (erythrophagocytic) macrophages. (b) CD163 immunostain highlights these cells and negative images of intracytoplasmic erythrocytes can be noted (DAB)

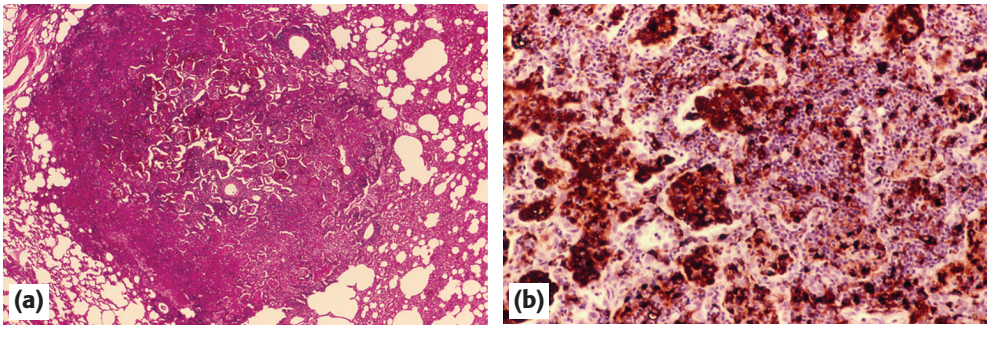

Fig. 16.6 Lung. (a) Nodular lesions with a peribronchial distribution are rarely seen in patients with HLH. These are not known to contain organisms after extensive search and culture. (b) Alveolar, but also interstitial, macrophages comprise the lesions (DAB, CD68)

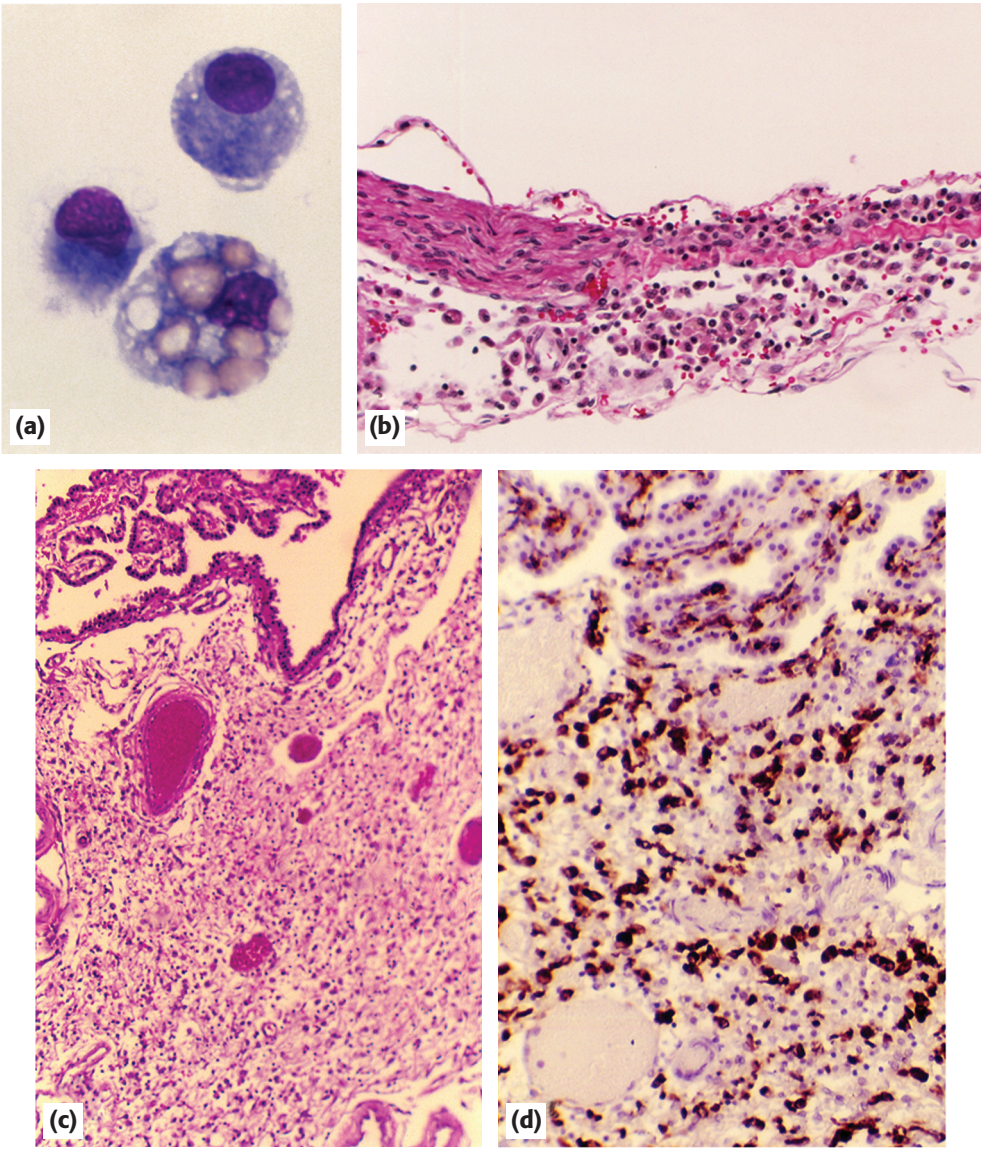

Fig. 16.7 CNS. (a) Spinal fluid. Monocytoid and hemophagocytic macrophages are a common finding in the CSF during active disease. (b) A spinal nerve root reveals the presence of macrophages within the leptomeninges. (c) Subchoroidal ventricular areas are a site for HLH infiltration. (d) Immunostaining for CD68 reveals the extensive macrophage presence in the area represented in (c) (DAB)

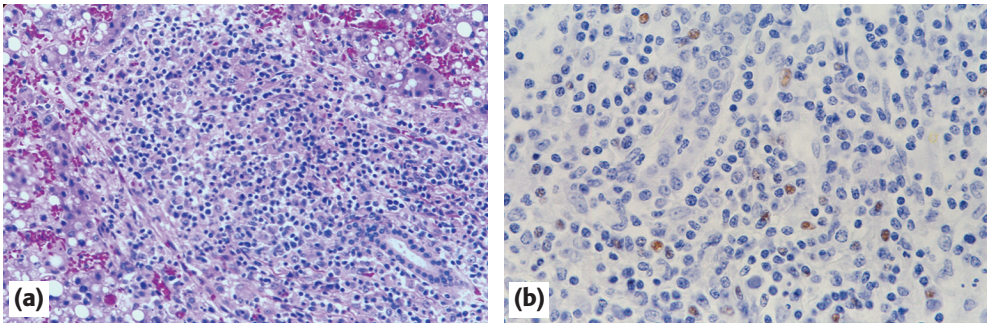

Fig. 16.8 EBV-related HLH, liver. (a) A mixed lymphohistiocytosis is seen that markedly expands the portal area. (b) EBER-1 probe highlights the intranuclear presence of EBV RNA in lymphocytic nuclei. This was not an instance of X-linked lymphoproliferative syndrome (XLPD) which usually has a more activated lymphoid presence, more EBV and greater hepatocellular necrosis

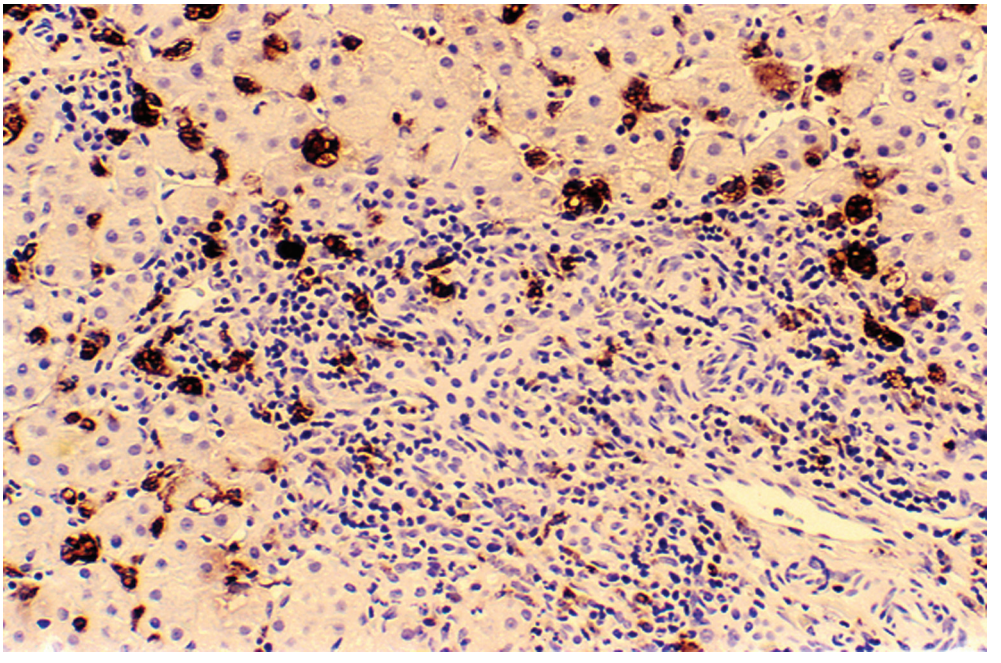

Fig. 16.9 Liver. Macrophage activation syndrome in a child with hepatitis shows the presence of phagocytic sinusoidal Kupffer cells, but lacks the presence of the portal macrophages typical of HLH (contrast with Figure 16.3(b)) (CD68, KP-1, DAB)